Available online at www.pelagiaresearchlibrary.com

Pelagia Research Library

Advances in Applied Science Research, 2011, 2 (6):83-100

ISSN: 0976-8610
CODEN (USA): AASRFC

Comparative assessment and result analysis of various control methods, applied on a rotary inverted pendulum, SRV 02 series

Md. Akhtaruzzaman* **and Amir A. Shafie**

Department of Mechatronics Engineering, Kulliyyah of Engineering, International Islamic University Malaysia, Kuala Lumpur, Malaysia

---

ABSTRACT

Inverted pendulum control is one of the fundamental problems in the field of control theory especially in the control of a walking robot. This paper describes the steps to design various controllers for a rotary motion inverted pendulum which was operated by a rotary servo plant, SRV 02 Series. The paper then compares the classical and modern control techniques used to design the control systems. Firstly, the most popular system, Single Input Single Output (SISO) system, was applied where 2DOF Proportional-Integral-Derivative (PID) compensator design was included. In this paper the common Root Locus Method is described step by step to design the two compensators of PID controller. Designing the control system using 2DOF PID is quiet challenging task for the rotary inverted pendulum because of its highly nonlinear and open-loop unstable characteristics. Secondly, the paper describes the two Modern Control techniques that include Full State Feedback (FSF) and Linear Quadratic Regulator (LQR). For the experiment, FSF and LQR control systems were tested both for the Upright and Swing-Up mode of the Pendulum. Finally, experimental and MATLAB based simulation results are described and compared based on the three control strategy which were designed to control the Rotary Inverted Pendulum. Both the simulated and experimental results show that the LQR controller presents better performance over the other two controllers.

Keywords : 2DOF PID, FSF, LQR, Inverted pendulum control.

INTRODUCTION

A modern control theory can be verified by the inverted pendulum control which can be considered as a very good example in control engineering. It is an excellent model for the plasma impact force sensor [1], attitude control of a space booster rocket and a satellite [2], an automatic aircraft landing system [2], aircraft stabilization in the turbulent air-flow [2], stabilization of a cabin in a ship [2]. This model also can be an initial step in stabilizing androids. The inverted pendulum is highly nonlinear and open-loop unstable system that makes control more challenging. It is an intriguing subject from the control point of view due to its intrinsic nonlinearity. Common control approaches such as *2DOF PID* controller, *FSF* control and *LQR*

requires a good knowledge of the system and accurate tuning in order to obtain desired performances. However, an accurate mathematical model of the process is often extremely complex to describe using differential equations. Moreover, application of these control techniques to a humanoid platform, which has more than one stage system, may result a very critical design of control parameters and difficult stabilization.

PID controller is a common control loop feedback mechanism which is generally used in industrial control system. It depends on three separate parameters, Proportional, Integral and Derivative, values where the Proportional indicates the response of the current error, the Integral value determines the response based on the sum of the recent errors and the Derivative value determines the response based on the rate of the changing errors. Finally the weighted sum of the three parameters is used to control the process or plant. Because of the simple structure, it is not an easy task to tune the *PID* controller to achieve the expected overshoot, settling time, steady state error etc. of the system behavior. Based on this issue several *PID* control techniques such as *I-PD* control system [3] [4], *2DOF PID* control system [3] [4] are introduced. The number of closed-loop transfer functions determines the degree of freedom of a control system where the transfer functions can be adjusted independently.

The analysis and design of feedback control system are carried out using transfer functions along with various tools such as root-locus plots, Bode plots, Niquist plots, Nichol's chart etc. These are the techniques in classical control theory where the classical design methods suffer from certain limitations because; the transfer function model is applicable only for linear time-invariant system and generally restricted to *SISO* system [8]. The transfer function technique reveals only the system output for a given input and it does not provide any information of internal behavior of the system. These limitations of the classical method have led to the development of state variable approach, direct time domain approach, which provides a basis of modern control theory. It is a powerful technique for the analysis and design of linear and nonlinear, time-invariant or time-varying multi-input, multi-output (*MIMO*) system.

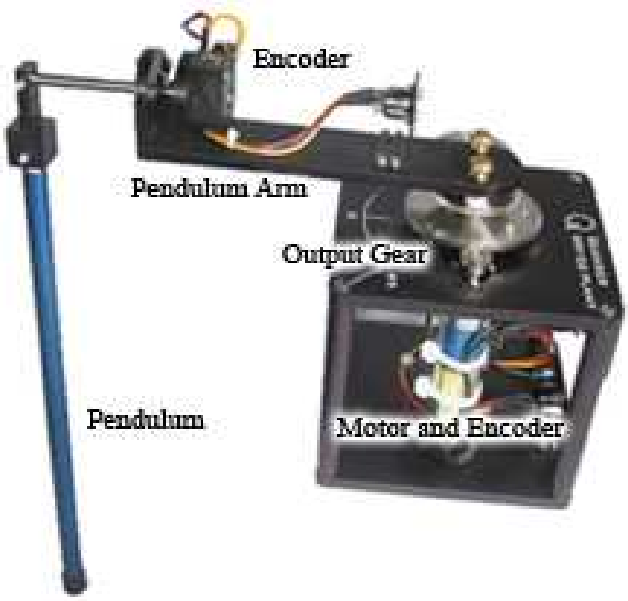

Figure 1: Rotary inverted pendulum model *SRV-02*.

FSF control also known as Pole Placement, is a method which is employed in state feedback control theory to place the closed-loop pools of a plant in pre-determined locations in the s-plan.

Placing pools is desirable because the location of the pools determines the eigenvalues of the system, which controls the characteristics of the system response. The *FSF* algorithm is actually an automated technique to find an appropriate state-feedback controller. Another alternative technique, *LQR* is also a powerful method to find a controller over the use of the *FSF* algorithm.

The rotary motion inverted pendulum, which is shown in Figure 1, is driven by a rotary servo motor system (*SRV-02*). The servo motor drives an independent output gear whose angular position is measured by an encoder. The rotary pendulum arm is mounted on the output gear. The pendulum is attached to a hinge instrumented with another encoder at the end of the pendulum arm. This second encoder measures the angular position of the pendulum. The system is interfaced by means of a data acquisition card and driven by Matlab / Simulink based real time software. The pendulum has two equilibrium points, stable and unstable. At the stable equilibrium point the rod is vertical and pointing down while an unstable equilibrium at the point where the rod is vertical and pointing up. In this paper the three methods, *2DOF PID*, *FSF* and *LQR*, are applied to design the controller of the rotary inverted pendulum.

In the section 2 of the paper presents the mathematical analysis and state space representation of the rotary inverted pendulum system. Various control strategies including the *2DOF PID*, *FSF* and *LQR* are designed and demonstrated in the section 3. Section 4 of the paper delineates the comparative assessment of the various results based on the simulation and practical experimentation of the designed controllers. Finally the section 5 draws the abridgement of the writings.

Mathematical modeling of rotary motion inverted pendulum

Figure 2 (a) shows the rotational direction of rotary inverted pendulum arm. Figure 2 (b) depicts the pendulum as a lump mass at half of the pendulum length. The pendulum is displaced with an angle α while the direction of θ is in the x-direction of this illustration. So, mathematical model can be derived by examining the velocity of the pendulum center of mass. The pendulum is considered as stable while the value of the pendulum angle is equal to zero or nearer to zero. This condition is maintained by controlling the velocity and direction of the arm's movement.

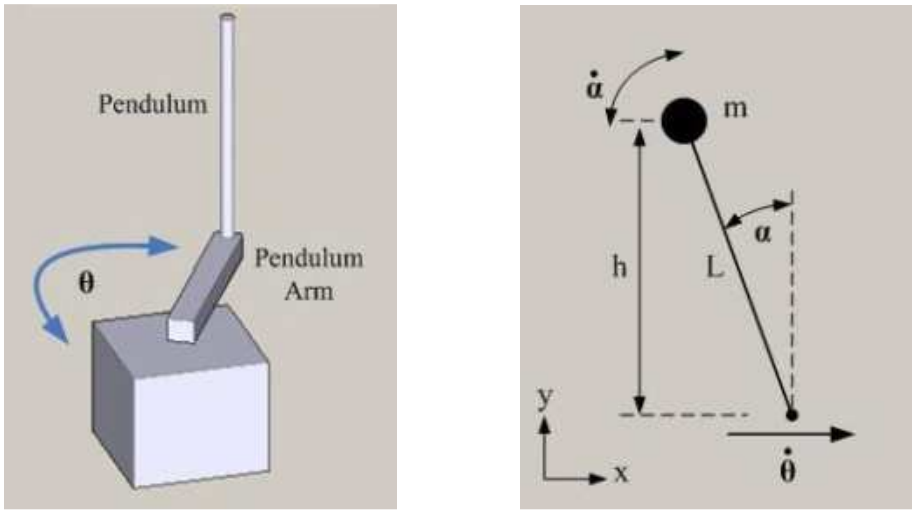

(a) Rotational direction of pendulum arm. *(b) Pendulum lump mass*

Figure 2: Pendulum motion and lump mass.

The following assumptions are made in modeling of the system:

- The system starts in a state of equilibrium meaning that the initial conditions are therefore assumed to be zero.
- The pendulum does not move more than a few degrees away from the vertical to satisfy a linear model.
- A small disturbance can be applied on the pendulum.

As the requirements of the design, the settling time, T_s, is to be less than 0.5 seconds, i.e. $T_s < 0.5secs$. The system overshoot value is to be at most 10%, i.e. $\%OP = 10$. The following table is the list of the terminology used in the derivations of system model.

Table 1: Symbols to describe equation parameters

Symbol	Description
L	Length to Pendulum's Center of Mass
m	Mass of Pendulum Arm
r	Rotating Arm Length V_x Velocity
θ	Servo load gear angle (radians)
α	Pendulum Arm Deflection (radians)
h	Distance of Pendulum Center of mass from ground
J_{cm}	Pendulum Inertia about its center of mass
V_x	Velocity of Pendulum Center of mass in the x-direction
V_y	Velocity of Pendulum Center of mass in the y-direction

There are two components for the velocity of the Pendulum lumped mass. So,

$$V_{\,Pen.\ center\ of\ mass} = -Lcos\,\alpha(\dot{\alpha})\hat{x} - Lsin\,\alpha(\dot{\alpha})\hat{y} \quad (1)$$

The pendulum arm also moves with the rotating arm at a rate of:

$$V_{\,arm} = r\dot{\theta} \quad (2)$$

The equations (1) and (2) can solve the x and y velocity components as,

$$V\,x = r\dot{\theta} - Lcos\,\alpha(\dot{\alpha}) \quad (3)$$

$$V\,y = -Lsin\,\alpha(\dot{\alpha}) \quad (4)$$

1.1 Deriving the system dynamic equations

Having the velocities of the pendulum, the system dynamic equations can be obtained using the Euler-Lagrange formulation.

1.1.1 Potential Energy

The only potential energy in the system is gravity. So,

$$V = P.E._{Pendulum} = mg\,h = mg\,Lcos\,\alpha \quad (5)$$

1.1.2 Kinetic Energy

The Kinetic Energies in the system arise from the moving hub, the velocity of the point mass in the x-direction, the velocity of the point mass in the y-direction and the rotating pendulum about its center of mass.

$$T = K.E._{Hub} + K.E._{Vx} + K.E._{Vy} + K.E._{Pendulum} \quad (6)$$

Since the modeling of the pendulum as a point at its center of mass, the total kinetic energy of the pendulum is the kinetic energy of the point mass plus the kinetic energy of the pendulum rotating about its center of mass. The moment of inertia of a rod about its center of mass is,

$$J_{cm} = \left(\frac{1}{12}\right) MR^2 \tag{7}$$

Since *L* is defined as the half of the pendulum length, *R* in this case would be equal to *2L*. Therefore the moment of inertia of the pendulum about its center of mass is,

$$J_{cm} = \left(\frac{1}{12}\right) MR^2 = \left(\frac{1}{12}\right) M(2L)^2 = \left(\frac{1}{3}\right) ML^2 \tag{8}$$

So, the complete kinetic energy, *T*, can be written as,

$$T = \left(\frac{1}{2}\right) J_{eq}\, \dot{\theta}^2 + \left(\frac{1}{2}\right) m \left(r\dot{\theta} - Lcos\, \alpha(\dot{\alpha}) \right)^2 + \left(\frac{1}{2}\right) m\left(-Lsin\, \alpha(\dot{\alpha})\right)^2 + \left(\frac{1}{2}\right) J_{cm}\, \dot{\alpha}^2 \tag{9}$$

After expanding the equation and collecting terms, the Lagrangian can be formulated as,

$$L = T - V = \left(\frac{1}{2}\right) J_{eq}\, \dot{\theta}^2 + \left(\frac{2}{3}\right) mL^2\dot{\alpha}^2 - mLr \cos \alpha(\dot{\alpha})(\dot{\theta}) + \left(\frac{1}{2}\right) mr^2\dot{\theta}^2 - mgLcos\, \alpha \tag{10}$$

The two generalized co-ordinates are θ and α. So, another two equations are,

$$\frac{\delta}{\delta t}\left(\frac{\delta L}{\delta \dot{\theta}}\right) - \frac{\delta L}{\delta \theta} = T_{output} - B_{eq}\dot{\theta} \tag{11}$$

$$\frac{\delta}{\delta t}\left(\frac{\delta L}{\delta \dot{\alpha}}\right) - \frac{\delta L}{\delta \alpha} = 0 \tag{12}$$

Solving the equations and linearizing about $\alpha = 0$, equations become,

$$\left(J_{eq} + mr^2\right)\ddot{\theta} - mLr\ddot{\alpha} = T_{output} - B_{eq}\dot{\theta} \tag{13}$$

$$\frac{4}{3}mL^2\ddot{\alpha} - mLr\ddot{\theta} - mgL\alpha = 0 \tag{14}$$

The output Torque of the motor which act on the load is defined as,

$$T_{output} = \frac{\eta_m \eta_g K_t K_g (V_m - K_G K_m \dot{\theta})}{R_m} \tag{15}$$

Finally, by combining the above equations, the following state-space representation of the complete system is obtained.

$$\begin{bmatrix} \dot{\theta} \\ \dot{\alpha} \\ \ddot{\theta} \\ \ddot{\alpha} \end{bmatrix} = \begin{bmatrix} 0 & 0 & 1 & 0 \\ 0 & 0 & 0 & 1 \\ 0 & \frac{bd}{E} & \frac{-cG}{E} & 0 \\ 0 & \frac{qd}{E} & \frac{-bG}{E} & 0 \end{bmatrix} \begin{bmatrix} \theta \\ \alpha \\ \dot{\theta} \\ \dot{\alpha} \end{bmatrix} + \begin{bmatrix} 0 \\ 0 \\ c\frac{\eta_m \eta_g K_t K_g}{R_m E} \\ b\frac{\eta_m \eta_g K_t K_g}{R_m E} \end{bmatrix} V_m \tag{16}$$

Here, $a = J_{eq} + mr^2$, $b = mLr$, $c = 4/3mL^2$, $d = mgL$, $E = ac - b^2$, $G = \frac{\eta_m \eta_g K_t K_m K_g^2 - B_{eq} R_m)}{R_m}$. The following table shows the typical configuration of the system.

Table 2: Typical configuration of the system

Symbol	Description	Value
K_t	Motor Torque Constant	0.00767
K_m	Back EMF Constant	00767
R_m	Armature Resistance	2.6
K_g	SRV02 system gear ratio (motor->load)	14 (14x1)
η_m	Motor efficiency	0.69
η_g	Gearbox efficiency	0.9
B_{eq}	Equivalent viscous damping coefficient	1.5 e-3
J_{eq}	Equivalent moment of inertia at the load	9.31 e-4

Based on the typical configuration of the *SRV02* & the Pendulum system, the above state space representation of the system is,

$$\begin{bmatrix} \dot{\theta} \\ \dot{\alpha} \\ \ddot{\theta} \\ \ddot{\alpha} \end{bmatrix} = \begin{bmatrix} 0 & 0 & 1 & 0 \\ 0 & 0 & 0 & 1 \\ 0 & 39.32 & -14.52 & 0 \\ 0 & 81.78 & -13.98 & 0 \end{bmatrix} \begin{bmatrix} \theta \\ \alpha \\ \dot{\theta} \\ \dot{\alpha} \end{bmatrix} + \begin{bmatrix} 0 \\ 0 \\ 25.54 \\ 24.59 \end{bmatrix} V_m \quad (17)$$

$$Y = \begin{bmatrix} 1 & 0 & 0 & 0 \\ 0 & 1 & 0 & 0 \end{bmatrix} \begin{bmatrix} \theta \\ \alpha \end{bmatrix} + \begin{bmatrix} 0 \\ 0 \end{bmatrix} V_m \quad (18)$$

2. Controller Design

2.1 Design of a *2DOF PID* controller

Based on the above state space equation it is possible to derive the following two transfer functions.

$$\frac{\theta_s}{V_m} = \frac{25.54\, s^2 - 4.537e{-}014\, s - 1122}{s^4 + 14.52\, s^3 - 81.78\, s^2 - 638\, s} \quad (19)$$

$$\frac{\theta_s}{V_m} = \frac{25.54\, s^2 - 4.537e{-}014\, s - 1122}{s^4 + 14.52\, s^3 - 81.78\, s^2 - 638\, s} \quad (20)$$

From these two transfer functions it is easy to derive another new transfer function which describes the behavior of α depending on the behavior of θ.

$$\frac{\alpha_s}{\theta_s} = \frac{24.59\, s + 0.00231}{25.54\, s^2 - 4.537e{-}014\, s - 1122} \quad (21)$$

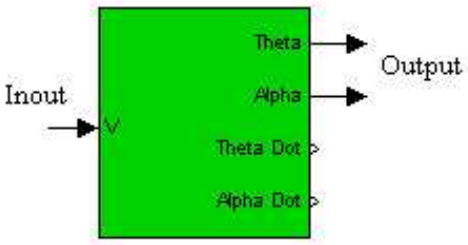

Figure 3: Plant model of *SRV-02* series.

Figure 3 shows the rotary inverted pendulum plant model where the pendulum arm position theta, θ, is regulated by the input voltage V. The main target is to maintain pendulum angle alpha, α, as zero so that the inverted pendulum remains stable. Here the output theta has the responsibility to do this job. So it is necessary to design two *PID* compensators where one will maintain the speed and position of theta while the other controller will function based on the feedback of alpha, α. The overall controller block diagram becomes as follows where $G(\theta)$ and $G(\alpha)$ indicates the plant model of θ and α output while $C(\theta)$ and $C(\alpha)$ are the two *PID* compensators respectively.

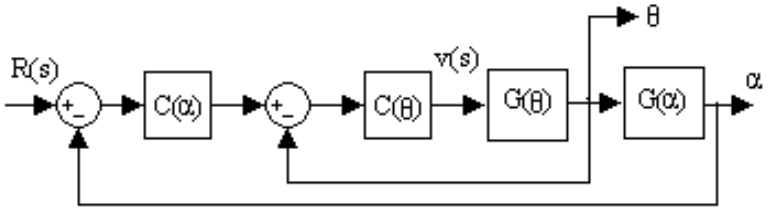

Figure 4: *2DOF PID* controller block diagram.

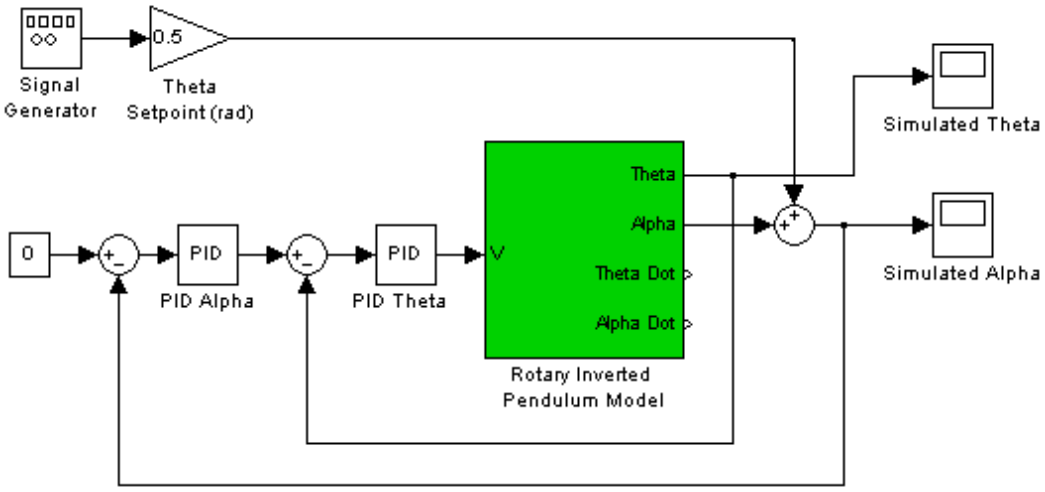

Figure 5: Block diagram of *2DOF PID* controller for rotary inverted pendulum model.

2.1.1 Root Locus analysis

From the design requirements, the settling time, $T_s = 0.5$ sec and the percentage of over shoot, $\%OP = 10$. Based on the specification it is important to determine the dominant pole on the root locus plot. To determine the damping ration (ζ) and natural frequency (ω), the following equations are necessary.

$$\%OS = 100.e^{((-\pi\zeta)/\sqrt{(1-\zeta^2)})} \quad (22)$$

$$T_s = 4/(\omega.\zeta) \quad (23)$$

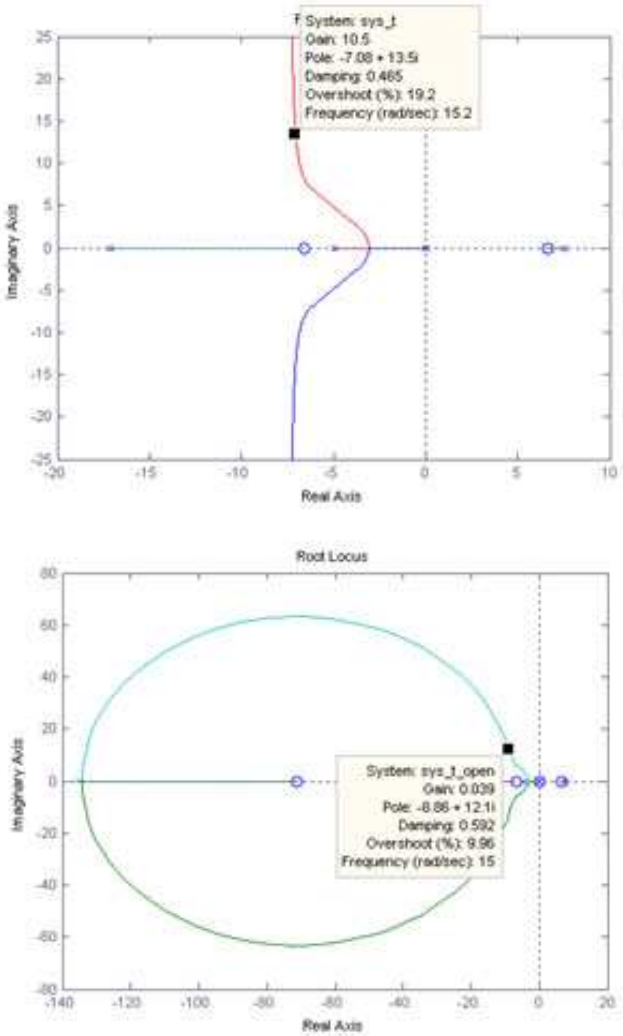

(a) Root locus plot for G(θ). *(b) Root locus plot for [G(θ) x C(θ)].*

Figure 6: Root locus plot for *G(θ)* and open loop [*G(θ) x C(θ)*].

So, $\zeta = 0.59116$ and $\omega = 13.5328$ rad/sec. To get settling time less than 0.5 sec, it needs to increase the value of ω. So, ω can be chosen as 15 rad/sec. Since it is already know the value of ω and ζ, so it can be determined the dominant pole by using equation below,

$$S_{1,2} = -\zeta.\omega \pm j\left(\omega.\sqrt{1-\zeta^2}\right) \quad (24)$$

$$= -8.86733 + 12.0984\text{i}$$

Based on the root locus design method, the desired pole is said on the root locus only and if only it fulfills the angle criterion which is determine by following equation,

$$\sum \angle Zeros - \sum \angle Poles = 180^o + 360^o(l-1) \quad (25)$$

Figure 6 (a) shows the root locus plot for *G(θ)* where it is clear that the dominant pole is not on the root locus. So, it needs to design a compensator, *C(θ)*, so that the dominant pole comes on the root locus. Here *C(θ)* indicates the *PID* compensator for the transfer function, (*θs/Vm*). Figure 6 (b) shows the root locus diagram after designing the first *PID*, *[G(θ) x C(θ)]*, where the dominant pole is on the root locus.

The corresponding gains *kp(θ)*, *ki(θ)* and *kd(θ)* are as 264.1355, 0.26413 and 3.7141 respectively. Basically it is a trial and error method where the values of damping ration, ζ, and frequency, ω, have to choose sometimes higher than the calculated one to meet the desired requirements. A small program is written based on the Root Locus algorithm where the program takes the values for ζ and ω to calculate the corresponding gains for both of the compensators. The calculated gains, *kp(α)*, *ki(α)* and *kd(α)*, are as 104.8795, 0.1049 and 0.4393 respectively for the second compensator *C(α)*.

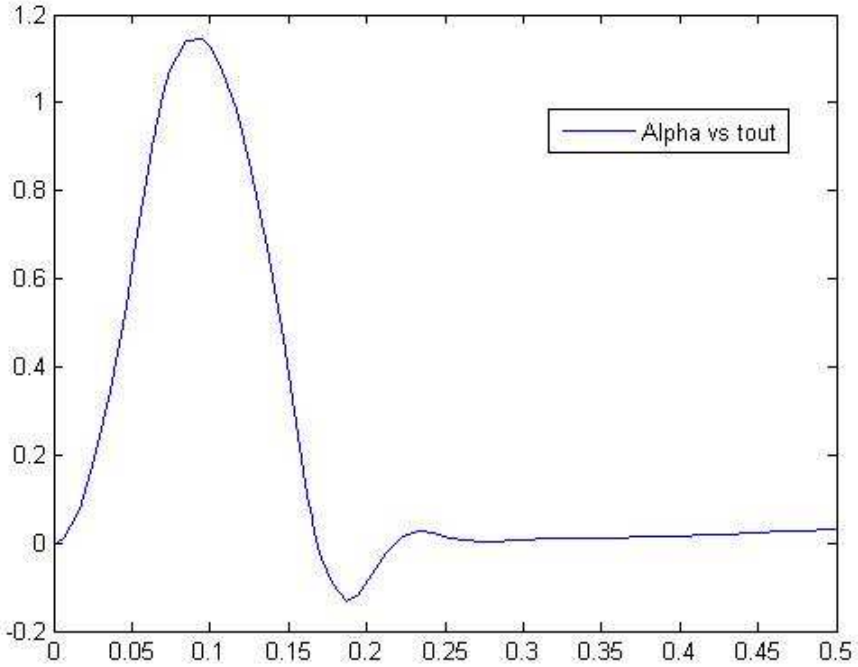

Figure 7: Unit step response of alpha for *2DOF PID* controller.

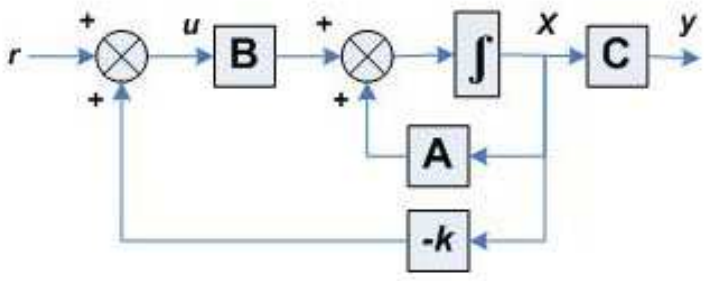

Figure 8: Block diagram of *FSF* controller.

2.2 Design of a *FSF* controller based on Ackerman's formula

In modern control system, state x is used as feedback instead of plant output y and k indicates the gain of the system. To design a *FSF* controller Ackerman's formula is used which is an easy and

effective method in modern control theory to design a controller via pole placement technique. Figure 8 shows a basic block diagram of a *FSF* controller of a system.
Ackerman's formula is represented as,

$$K = [0 \cdots 0\ 1]M_c^{-1}\emptyset_d(A) \quad (26)$$

$$M_c = \begin{bmatrix} B & AB & \cdots & A^{(n-1)}B \end{bmatrix} \quad (27)$$

Where M_C indicates the controllability matrix and $\Phi_d(A)$ is the desired characteristic of the closed-loop poles which can be evaluated as $s=A$. The close loop transfer function is selected based on *ITAE* table, shown in figure 9, and the value of frequency is taken as 10 rad/s.

$$s^2 + 3.2\omega_0 s + \omega_0^2$$
$$s^3 + 1.75\omega_0 s^2 + 3.25\omega_0^2 s + \omega_0^3$$
$$s^4 + 2.41\omega_0 s^3 + 4.93\omega_0^2 s^2 + 5.14\omega_0^3 s + \omega_0^4$$
$$s^5 + 2.19\omega_0 s^4 + 6.50\omega_0^2 s^3 + 6.30\omega_0^3 s^2 + 5.24\omega_0^4 s + \omega_0^5$$
$$s^6 + 6.12\omega_0 s^5 + 13.42\omega_0^2 s^4 + 17.16\omega_0^3 s^3 + 14.14\omega_0^4 s^2 + 6.76\omega_0^5 s + \omega_0^6$$

Figure 9: *ITAE* characteristic equation table.

As the denominator of the transfer function of $\theta s/Vm$ is a fourth order polynomial, from the *ITAE* table the characteristics equation will be,

$$S^4+21S^3+340S^2+2700\ S+10000 = 0 \quad (28)$$

The controller matrix gain can be calculated using the following *MATLAB* code,

```
A= [0 0 1 0;0 0 0 1;0 39.32 -14.52 0;0 81.78 -13.98 0];
B = [0; 0; 25.54; 24.59];
a = [1 21 340 2700 10000];
P = roots(a);
K= ACKER(A, B, P);
```

So the gain matrix becomes,

$$K = (-8.9144\ \ 26.4116\ \ -2.9755\ \ 3.3539) \quad (29)$$

Using this *K* and the control law, $u = -Kx$, the system is stabilized around the linearized point (pendulum upright). The state feedback optimal controller is only effective when the pendulum is near the upright position. In the plant model of the rotary inverted pendulum, the output theta (θ) is regulated by the input voltage (V). Here theta has the responsibility to keep the inverted pendulum vertically upright where alpha (α) will be zero. Figure 10 shows the controller block diagram to control the pendulum from the upright position.

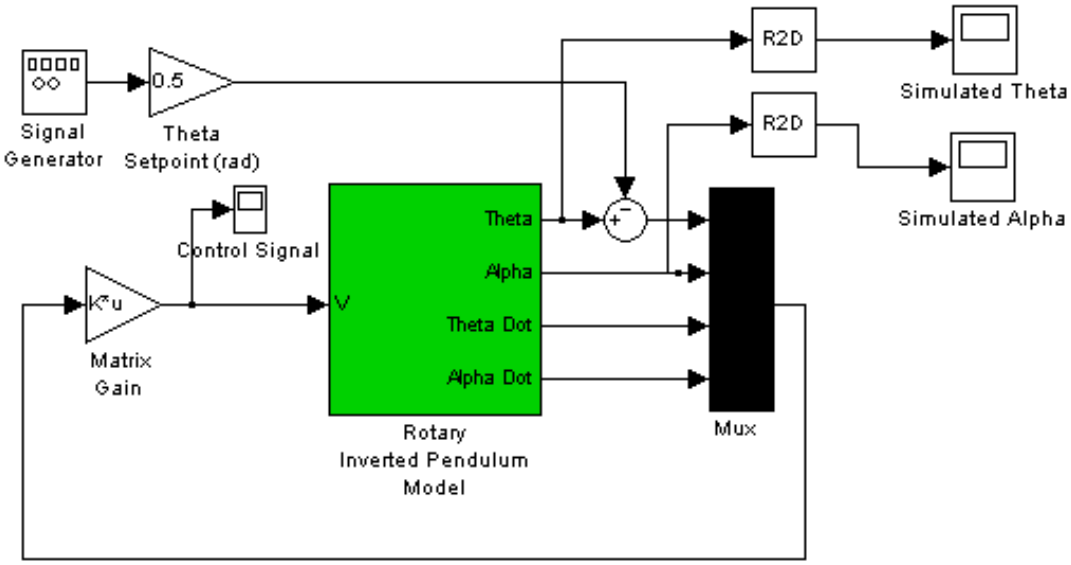

Figure 10: Controller Block Diagram (Upright mode).

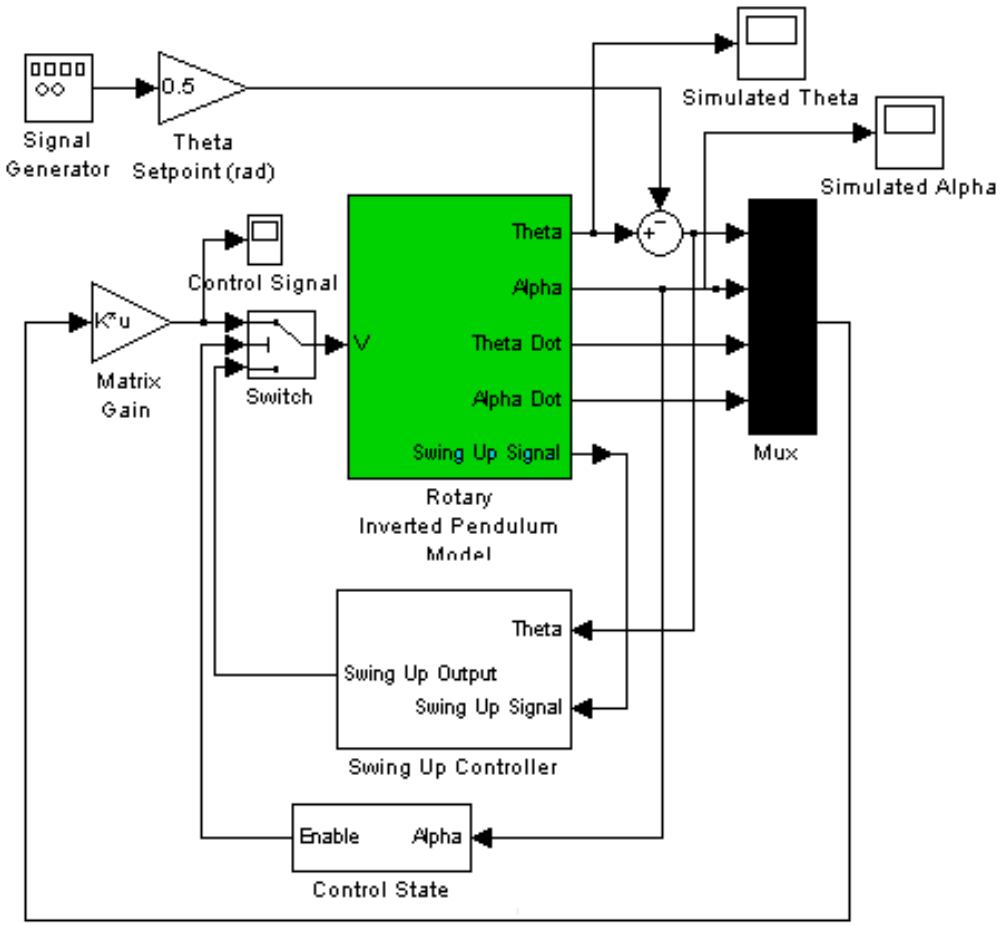

Figure 11: Controller Block Diagram (swing-up mode).

Figure 11 shows the block diagram of the controller for the swing up mode. The pendulum starts from down words position and whenever it comes to the upright mode the full state feedback controller will maintain the pendulum in that position and make it stable.

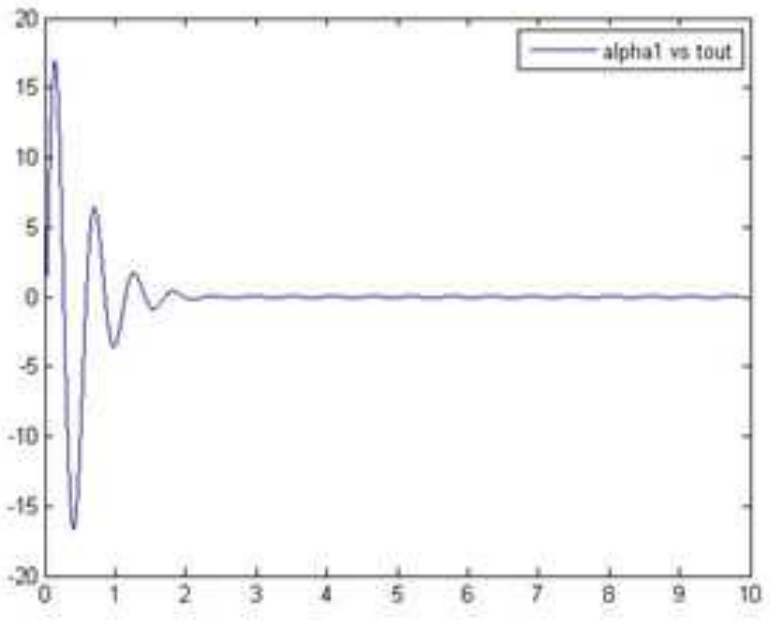

Figure 12: Step response of alpha in *FSF* controller.

2.3 Controller design using LQR technique

Linear Quadratic Regulator (*LQR*) is design using the linearized system. In a *LQR* design process, the gain matrix *K*, for a linear state feedback control law, u = -*Kx*, is found by minimizing a quadratic cost function of the form as,

$$j = \int_0^\infty x(t)^T Q x(t) + u(t)^t \, Ru(t) dt \qquad (30)$$

Here Q and R are weighting parameters that penalize certain states or control inputs. In the design the weighting parameters of the optimal state feedback controller are chosen as,

$$Q = \begin{pmatrix} 6 & 0 & 0 & 0 \\ 0 & 1 & 0 & 0 \\ 0 & 0 & 1 & 0 \\ 0 & 0 & 0 & 0 \end{pmatrix} \qquad (31)$$

$$R = 1 \qquad (32)$$

In this design, the controller gain matrix, *K*, of the linearized system is calculated using *MATLAB* function. Basically this method is another powerful technique to calculate the gain matrix which is applied in the same model using in *FSF* controller design.

$$K = (-2.4495 \quad 27.5843 \quad -2.5505 \quad 3.9200) \qquad (33)$$

Here the selected diagonal matrix, Q is chosen where the values of q_{11}, q_{22}, q_{33} and q_{44} are 6, 1, 1 and 0 respectively. The diagonal values are selected based on iterative method. It is found that the diagonal values for q_{11} and q_{22} are more sensitive than others. Output performances are tested based on four different values of the matrix Q. The test cases of Q matrix are shown in the table bellow,

Table 3: Test cases of the diagonal matrix, *Q*.

Test case	Diagonal matrix, Q
1	$Q_1 = \begin{pmatrix} 6 & 0 & 0 & 0 \\ 0 & 01 & 0 & 0 \\ 0 & 0 & 1 & 0 \\ 0 & 0 & 0 & 0 \end{pmatrix}$
2	$Q_2 = \begin{pmatrix} 1 & 0 & 0 & 0 \\ 0 & 01 & 0 & 0 \\ 0 & 0 & 1 & 0 \\ 0 & 0 & 0 & 1 \end{pmatrix}$
3	$Q_3 = \begin{pmatrix} 6 & 0 & 0 & 0 \\ 0 & 10 & 0 & 0 \\ 0 & 0 & 1 & 0 \\ 0 & 0 & 0 & 0 \end{pmatrix}$
4	$Q_4 = \begin{pmatrix} 5 & 0 & 0 & 0 \\ 0 & 20 & 0 & 0 \\ 0 & 0 & 0 & 0 \\ 0 & 0 & 0 & 0 \end{pmatrix}$

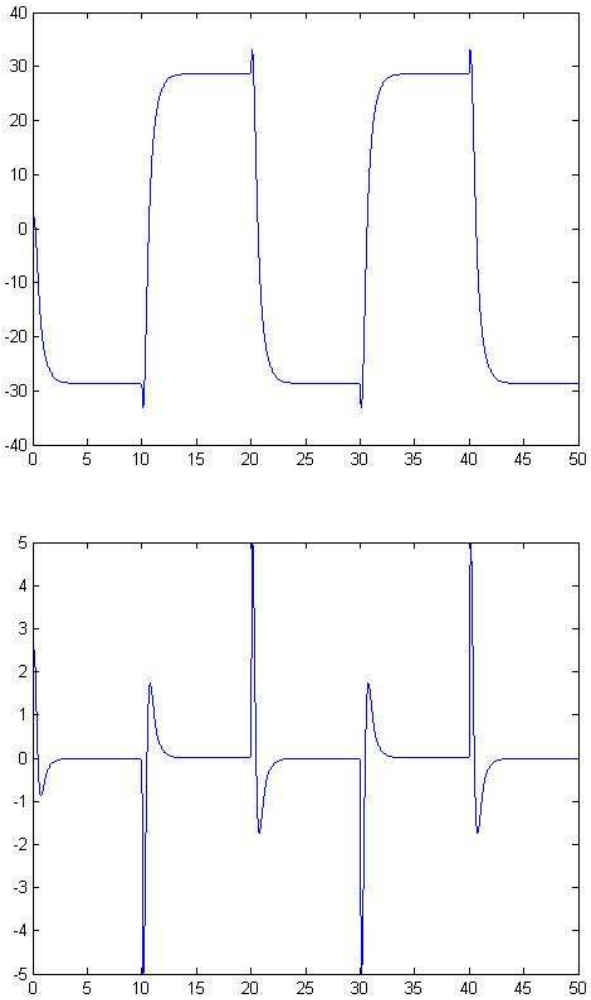

(a) Unit step response of theta (b) Unit step response of alpha.

Figure 13: Unit step response of theta and alpha for *LQR* controller.

Figure 13(a) and 13(b) show the simulated output of theta and alpha based on the *Q1* matrix where diagonal values are 6, 1, 1 and 0 (test 1). From the results of other test cases, it is clearly identified that the settling time of theta for test *Q1* is less. Though the alpha overshoot and settling time for test *Q2* is smaller to test *Q1*, still the performance of the test *Q1* is better than other because of the settling time. In practical case the test *Q1* result also shows the better performance.

3. COMPARATIVE ASSESSMENT AND ANALYSIS OF THE RESULTS

Figure 14 shows the experimental result of theta and alpha while *2DOF PID* controller tries to maintain the system stability. In the practical case the controller is capable to maintain the pendulum vertically up but it is not robust. The other two controllers (*FSF* and *LQR*) can be considered as robust. For both of the controllers, *FSF* and *LQR*, comparative simulated results of theta and alpha are shown in the figure 15 (a) and 15 (b) respectively.

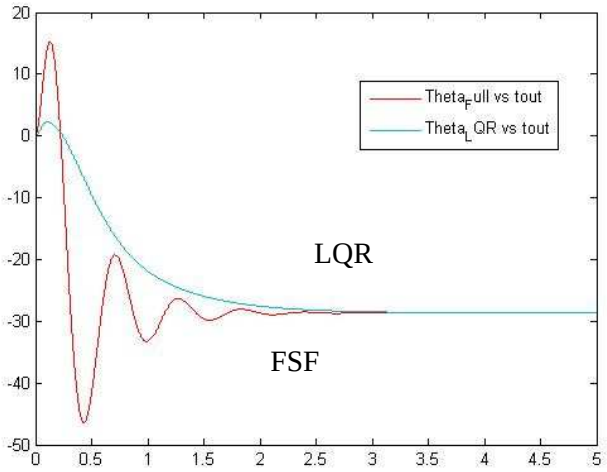

(a) Comparative results of theta.

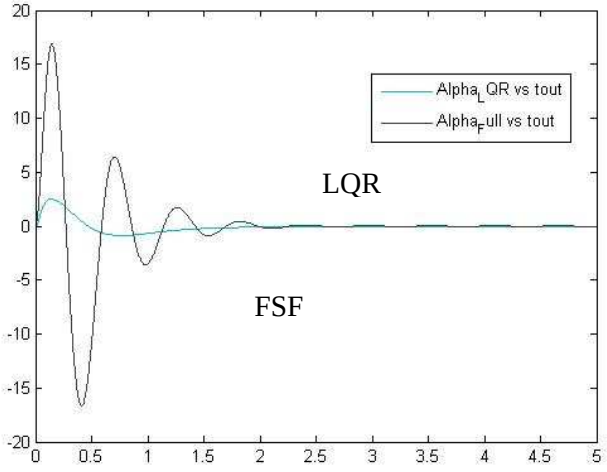

(b) Comparative results of alpha.

Figure 15: Comparative results of theta and alpha for both *FSF* and *LQR* controllers.

From the figure 15 it is clearly seen that for both of the outputs, theta and alpha, *LQR* controller shows the better result where rising time, settling time, overshoot and steady state error are more acceptable than *FSF* controller. Figure 16 shows the experimental result of *LQR* controller.

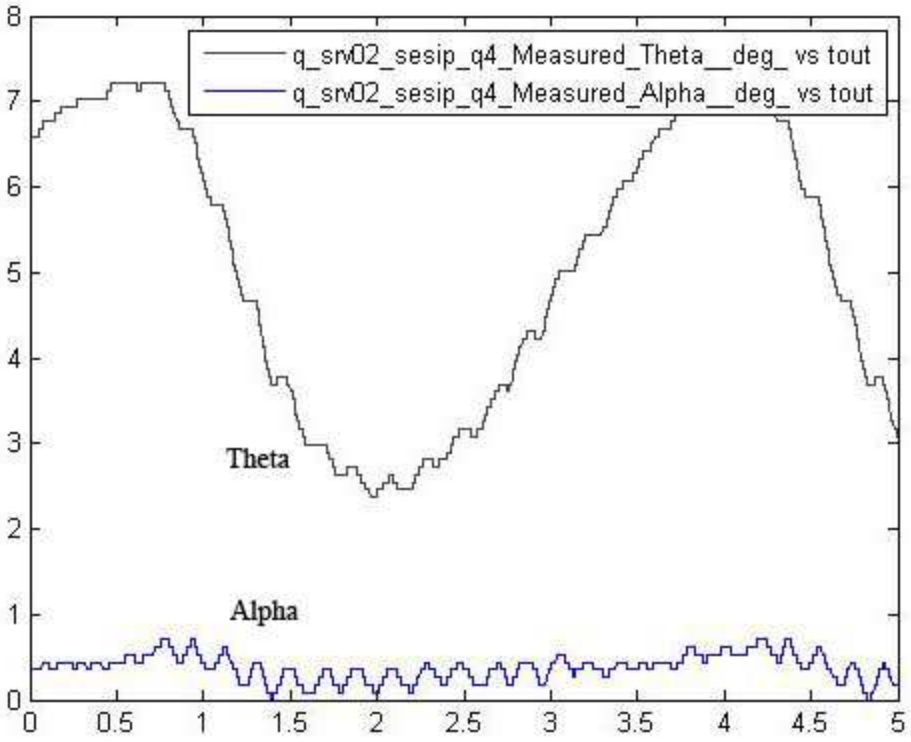

Figure 16: Experimental result of the pendulum based on *LQR* controller.

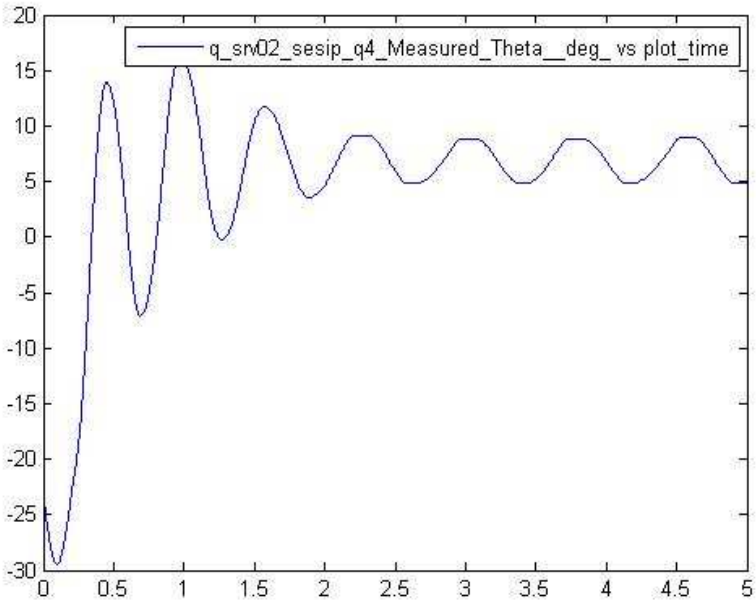

(a) Experimental result of theta.

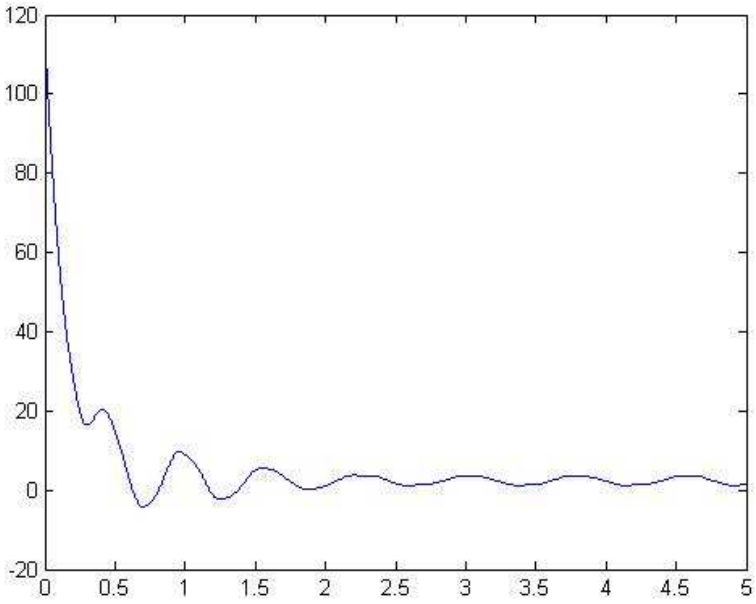

(b) Experimental result of alpha.

Figure 17: Experimental results of the pendulum based on *FSF* controller.

The experimental results of theta and alpha for *FSF* controller are presented in the Figure 17. By comparing the two experimental results shown in Figure 16 and Figure 17, it can be said that the stability of *LQR* controller is more than the *FSF* controller because the overshoot of alpha for *LQR* is smaller than the overshoot for *FSF* controller. *LQR* also tries to keep the value of pendulum angle as nearer as zero than the other. Based on the simulated results of unit step response of alpha for all the three controllers, *2DOF PID*, *FSF* and *LQR*, a comparison table shown in the Table 4, can be drawn to represent the characteristics of output through which a better controller can be identified.

Table 4: Comparison of unit step response for pendulum angle, alpha.

	Rising time	Settling time	Overshoot range	Steady-state error
2DOF PID	0.1	0.23	0.15 to -0.13	0.02
FSF	0.16	1.24	16.8 to -16.6	-0.004
LQR	0.14	0.39	2.5 to 0.86	-0.0003

CONCLUSION

Based on the result, shown in Table 4, the classical control method, *2DOF PID*, is capable to control the nonlinear system especially the rotary inverted pendulum. The simulated unit response characteristics of *2DOF PID* controller are satisfactory but in practical it is not robust. The performance of *2DOF PID* can be improved by tuning the controller parameters. Simulation and experimental studies determine the efficiency, reliability and accuracy of other two controllers, *FSF* and *LQR*. The controllers are not only meet the design requirements but also robust to the parameter variations. The *LQR* controller is more robust and reliable than the FSF controller in successfully swinging the pendulum to the upright position. As the data indicates, the *LQR* controller is also faster than the *FSF* controller. Overall, it is seen that the *LQR* controller is more convenient to swing up the pendulum to its upright mode and maintain stability on the unstable equilibrium point. From the experimental results it is considered,

however, that both controllers (*FSF* and *LQR*) can be effective in maintaining the rotary inverted pendulum stable.

Acknowledgements
The authors would like to thank their honorable parents. They are also grateful to Dr. Wahyudi Martono (late), who was with the Department of Mechatronics Engineering, International Islamic University Malaysia (IIUM). Most importantly the authors would like to express their gratitude to the Ministry of Higher Education (MOHE), Malaysia, in funding the project through the Fundamental Research Grant Scheme (FRGS).

REFERENCES

[1]Longmier BW, Bering EA, Squire JP, Glover TW, Chang-Díaz FR, Brukardt M, Hall Thruster and VASIMR VX-100 Force measurements using a Plasma Momentum Flux Sensor, *47th AIAA Aerospace Sciences Meeting Including the New Horizons Forum and Aerospace Exposition*, 5-8 January **2009**, Orlando, Florida, pp 1-13.
[2]Nasir ANKB, *Modeling and controller design for an inverted pendulum*, MSc. Thesis, UTM, Malaysia, April **2007**.
[3]Yukitomo M, Shigemasa T, Baba Y, Kojima F, A Two Degrees of Freedom PID Control System, its Features and Applications, *Proceeding of 5th Asian Control Conference* **2004**, pp 456-459.
[4]Mueller RL, The Inverted Pendulum Problem as a Senior Design Project, *Proceedings of the* **2004** *American Society for Engineering Education Annual Conference & Exposition*, **2004**.
[5]Purtojo, Akmeliawati R, Wahyudi, Two-parameter Compensator Design for Point-to-point (PTP) Positioning System Using Algebraic Method, *The Second International Conference on Control, Instrumentation and Mechatronic Engineering (CIM09), June 2-3,* **2009**, Malacca, Malaysia, pp 185 - 189.
[6]Giron-Sierra JM, *IEEE transactions on education, vol. 44, No.2,* may **2001**, pp 144-150.
[7]Araki M, Taguchi H, *International Journal of Control, Automation and Systems Vol. 1, No. 4,* December **2003**, pp 401-411.
[8]Gopal M, *Digital Control and State Variable methods Conventional and Neural-Fuzzy Control System*, 2nd edition, International Edition **2004**, Mc Graw Hill, Printed in Singapore.
[9]Akhtaruzzaman M, Samsuddin NB, Umar NB, Rahman M, Design and Development of a Wall Climbing Robot and its Control System. *Proceedings of 12th International Conference on Computer and Information Technology (ICCIT)*, December 21-23, **2009**, Independent University, Bangladesh, pp 309-313.
[10] Akhtaruzzaman M, Akmeliawati R, Yee TW, Modeling and Control of a Multi degree of Freedom Flexible Joint Manipulator. *Proceedings of the Second International Conference on Computer and Electrical Engineering (ICCEE)*, December 28-30, **2009**, Dubai, UAE, pp 249-254.
[11] Akhtaruzzaman M, Shafie AA, Rashid M, *Journal of Mechanical Engineering and Automation (JMEA)*, Scientific & Academic Publishing, **2011**.
[12] Akhtaruzzaman M, Razali NABM, Rashid MM, Shafie AA, *Journal of Applied Mechanics and Materials Vols. 110-116*, Trans Tech Publications, Switzerland, **2012**. pp 4941-4950.
[13] Akhtaruzzaman M, Shafie AA, Geometrical Analysis on BIOLOID Humanoid System Standing on Single Leg. *Proceedings of* **2011** *4th International Conference on Mechatronics (ICOM `11)*, 17-19 May **2011**, Kuala Lumpur, Malaysia.
[14] Akhtaruzzaman M, Shafie AA, An Attempt to Develop a Biped Intelligent Machine BIM-UIA. *Proceedings of* **2011** *4th International Conference on Mechatronics (ICOM `11)*, 17-19 May **2011**, Kuala Lumpur, Malaysia.

[15] Akhtaruzzaman M, Shafie AA, A Novel Gait for Toddler Biped and its Control Using PIC 16F877A. *Proceedings of* **2011** *4th International Conference on Mechatronics (ICOM `11)*, 17-19 May **2011**, Kuala Lumpur, Malaysia.
[16] Akhter MA, *Accumulation of Research*. LAP Lambert Academic Publishing, **2011**.
[17] Wu TY, Yeh TJ, Hsu BH, *The International Journal of Robotics Research (IJRR),* 19 January **2011**, pp 1-20.
[18] Sreekanth S, Venkataramana S, Rao GS, Saravana R, *Advances in Applied Science Research, Vol. 2, Issue 5,* **2011**. pp 185-196.
[19] Prasad BH, Ramacharyulu NCP, *Advances in Applied Science Research, Vol. 2, Issue 5,* **2011**. pp 197-206.
[20] Behera LK, Sasidharan A, *Advances in Applied Science Research, Vol. 2, Issue 3,* **2011**. pp 476-482.
[21] Egbai JC, *Advances in Applied Science Research, Vol. 2, Issue 4,* **2011**. pp 132-137.
[22] Nhivekar GS, Mudholkar RR, *Advances in Applied Science Research, Vol. 2, Issue 4,* **2011**. pp 410-416.
[23] Narsimlu G, Babu LA, Reddy PR, *Advances in Applied Science Research, Vol. 2, Issue 5,* **2011**. pp 416-420.
[24] Peter EE, *Advances in Applied Science Research, Vol. 2, Issue 5,* **2011**. pp 449-456.
[25] Yao LC, Chen JS, Hsu CY, *International Journal of Engineering, Vol. 1, Issue (1),* **2007**, pp 39-53.
[26] Mondal S, Nandy A, Chandrapal, Chakraborty P, Nandi GC, *International Journal of Robotics and Automation (IJRA), Vol. (2), Issue (2),* **2011**, pp 93-106.
[27] Kawarazaki N, Umeda S, Yoshidime T, Nishihara K, *Journal of Key Engineering Materials, Vol. 464,* **2011**, Trans Tech Publications, Switzerland, pp 111-114.